

MLSE Receiver for Direct-Sequence Spread-Spectrum Systems on a Multipath Fading Channel

Kai Tang, *Member, IEEE*, Laurence B. Milstein, *Fellow, IEEE*, and Paul H. Siegel, *Fellow, IEEE*

Abstract—To accommodate high-speed data transmissions, it may be necessary to substantially reduce the processing gain of a direct-sequence spread-spectrum (DSSS) system. As a result, intersymbol interference effects may become more severe. In this paper, we present a new structure for maximum-likelihood sequence estimation equalization of DSSS signals on a multipath fading channel that performs the function of despreading and equalization simultaneously. Analytical upper bounds are derived for the bit-error probability when random spreading sequences are used, and comparisons to simulation results show that the bounds are quite accurate. The results also show that significant performance improvement over the conventional RAKE receiver is obtained.

Index Terms—Direct-sequence spread spectrum (DSSS), fading channels, intersymbol interference (ISI), maximum-likelihood sequence estimation (MLSE).

I. INTRODUCTION

IN third-generation wireless land mobile communication systems, support of high-speed data transmission is required. In a wideband direct-sequence code-division multiple-access (DS-CDMA) system, high data rates can be accommodated by reducing the processing gain due to the spreading. When the spreading factor is sufficiently low (e.g., four), there is often only one high-data-rate user active in the system [1], [2]. Therefore, the multiple access interference (MAI) is low, but the intersymbol interference (ISI) due to the multipath fading channel might cause significant performance degradation to the conventional RAKE receiver, as shown in [3]. As a consequence, there is a need for equalization of DS signals with low processing gain.

Several attempts have been made to solve this problem. Since long spreading sequences are used in almost all practical CDMA systems, there is no cyclostationary property in the ISI component and a symbol-based minimum mean-square error (MMSE) receiver cannot be used. A linear chip equalizer, described in [4], tries to invert the channel transfer function

prior to the despreading. The advantage of this scheme is that the chip equalizer receiver also suppresses MAI in the synchronously transmitted downlink if orthogonal spreading sequences are employed. However, for channels with severe amplitude distortion, linear equalization leads to a substantial noise enhancement, which limits the application of this scheme. A RAKE maximum-likelihood sequence estimator (MLSE) receiver has been proposed in [5]. This suboptimal receiver consists of a conventional RAKE receiver, followed by an MLSE which tries to remove the ISI components in the RAKE combined signal. Its performance is evaluated in [5] by computer simulations, and significant improvement over the conventional RAKE receiver is observed. In this paper, we consider an optimal receiver structure, which is essentially an MLSE receiver operating at the chip rate. Note that a simplified chip-based MLSE multiuser detector was proposed in [6] and [7].

The optimal receiver for estimating an uncoded signal corrupted by ISI and additive white noise is a Viterbi decoder which performs MLSE on the ISI trellis [8], [9]. The performance of the MLSE has been analyzed thoroughly in [8] for time-invariant channels, and later in [10] for slowly time-varying multipath Rayleigh fading channels. In this paper, we show that if the spreading is treated as a special operation of encoding, the DS signal in the presence of ISI can be modeled by a single finite-state machine. The MLSE receiver operating on the combined trellis will jointly despread the signal and perform equalization. The performance of the MLSE receiver can be analyzed with the help of the error-state diagram [11]. However, for DS signals with long pseudorandom spreading sequences, the labels on the error-state diagram are time varying. It is shown in this paper how to incorporate the randomness of the spreading sequences into the analysis. As examples, we study both the two-tap and three-tap Rayleigh fading channels in detail.

The paper is organized in the following manner. In Section II, the system model is described. The structure of the MLSE receiver is presented in Section III, and two upper bounds on the bit-error probability of the receiver are derived in Section IV. In Section V, the two-tap and three-tap ISI channels are considered, and bounds on the performance are computed in detail. Finally, conclusions are drawn in Section VI.

II. SYSTEM MODEL

We consider a direct-sequence spread-spectrum (DSSS) system with both binary spreading and binary phase-shift

Paper approved by H. Leib, the Editor for Communication and Information Theory of the IEEE Communications Society. Manuscript received October 16, 2001; revised September 17, 2002. This work was supported in part by the National Science Foundation under Grant NCR-9725568, in part by the CoRe program of the State of California, in part by the Center for Wireless Communications, University of California, San Diego, and in part by the TRW Foundation.

K. Tang was with the University of California, San Diego, La Jolla, CA 92093 USA. He is now with Qualcomm, Inc., San Diego, CA 92121-1714 USA (e-mail: ktang@qualcomm.com).

L. B. Milstein and P. H. Siegel are with the Department of Electrical and Computer Engineering, University of California, San Diego, La Jolla, CA 92093-0407 USA (e-mail: milstein@ece.ucsd.edu; psiegel@ece.ucsd.edu).

Digital Object Identifier 10.1109/TCOMM.2003.814202

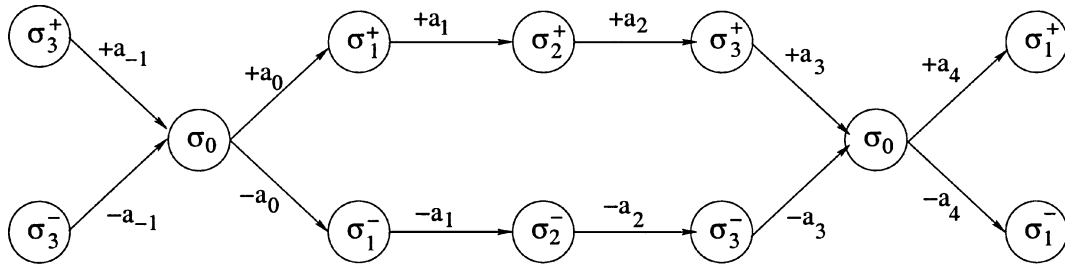


Fig. 1. Trellis of DSSS signal with BPSK data symbols, $N_s = 4$.

keying (BPSK) data symbols. Using a complex, baseband equivalent model, the transmitted signal may be expressed as

$$s(t) = \sqrt{2P}a(t)b(t)e^{j(\omega_c t + \phi)} \quad (1)$$

where P is the signal power, ω_c is the carrier frequency, and ϕ is the carrier phase. The spreading waveform $a(t)$ is given by $a(t) = \sum_{i=-\infty}^{\infty} a_i p_{T_c}(t - iT_c)$, and the data waveform $b(t)$ is given by $b(t) = \sum_{n=-\infty}^{\infty} b_n p_{T_s}(t - nT_s)$, where $\{a_i\}$ and $\{b_n\}$ are the discrete signature sequence and discrete data sequence, respectively, $p_\tau(t)$ denotes a unit height rectangular pulse of duration τ , and T_c and T_s are the chip duration and symbol duration, respectively. The spreading ratio is $N_s = T_s/T_c$. For a long spreading sequence system, $\{a_i\}$ is modeled as a sequence of independent and identically distributed (i.i.d.) random variables taking on the values of -1 and $+1$ with equal probability. For a system with short sequences, the period of the spreading sequence is assumed to be N_s , i.e., $a_i = a_{(i \bmod N_s)}$. The data symbol sequence $\{b_n\}$ consists of independent BPSK (± 1) symbols with equal probability.

The multipath fading channel is modeled as an $(L + 1)$ -tap transversal filter with tap spacing equal to T_c . The baseband equivalent impulse response is given by

$$h(t) = \sum_{l=0}^L \alpha_l(t) e^{j\phi_l(t)} \delta(t - lT_c) \quad (2)$$

where the tap coefficients, $\alpha_l(t)e^{j\phi_l(t)}$, are modeled as independent zero-mean complex Gaussian random processes, which vary slowly in time. The received signal can be written as

$$r(t) = \sqrt{2P} \sum_{l=0}^L \alpha_l e^{j(\omega_c t + \psi_l)} a(t - lT_c) b(t - lT_c) + \eta(t) \quad (3)$$

where $\psi_l = \phi_l + \phi - \omega_c lT_c$, $\eta(t)$ is a low-pass equivalent, white complex Gaussian noise process with $(1/2)E[\eta(t_1)\eta^*(t_2)] = N_0\delta(t_1 - t_2)$.¹ The dependence of the α_l 's and ψ_l 's on time is dropped to reflect the slowly fading assumption.

After down-conversion, the received signal passes through a chip-matched filter with a normalizing factor of $1/\sqrt{2PT_c}$. The i th output sample of the chip-matched filter is

$$r_i = \sum_{l=0}^L z_l a_{i-l} b_{\lfloor (i-l)/N_s \rfloor} + \eta_i \quad (4)$$

¹Following the conventional notation, z^* represents the conjugate of the complex variable z , and \mathbf{z}^H represents the complex conjugate transpose of the complex vector \mathbf{z} .

where $z_l \triangleq \alpha_l e^{j\psi_l}$ is a zero-mean complex Gaussian random variable, with variance $\Omega_l^2 = (1/2)E\{|z_l|^2\}$ described by the channel multipath intensity profile (MIP), $\mathbf{\Omega}^2 = \text{diag}\{\Omega_0^2, \Omega_1^2, \dots, \Omega_L^2\}$, and η_i is a zero-mean complex Gaussian random variable with variance $\sigma_\eta^2 = (1/2)E\{|\eta_i|^2\} = N_s N_0 / 2E_s$, where $E_s = PT_s$.

III. MLSE RECEIVER

Assume that M -symbol messages are transmitted over the channel. The MLSE receiver [8] finds the candidate sequence of information symbols $\{b_n\}_{n=0}^{M-1}$ that maximizes the likelihood of the received sequence $\{r_i\}_{i=0}^{MN_s+L-1}$. This is equivalent to maximizing the log-likelihood function which, neglecting constant scaling factors and additive terms, reduces to the form [12]

$$J(\{b_n\}) = \sum_{i=0}^{MN_s+L-1} \sum_{l=0}^L 2\Re\{r_i(z_l a_{i-l} b_{\lfloor (i-l)/N_s \rfloor})^*\} - \sum_{i=0}^{MN_s+L-1} \left| \sum_{l=0}^L z_l a_{i-l} b_{\lfloor (i-l)/N_s \rfloor} \right|^2. \quad (5)$$

If we treat the direct spreading as an $(N_s, 1)$ binary block code, the spreading operation can be characterized as a time-varying trellis with period N_s . Let σ_i be the state of the spreading "encoder" before $a_i b_{\lfloor i/N_s \rfloor}$ is transmitted. The combined trellis of the direct spreading and ISI channel can be viewed as generated by a finite-state machine [9], [13], whose states are given by $\xi_i \triangleq (\sigma_i; a_{i-L} b_{\lfloor (i-L)/N_s \rfloor}, \dots, a_{i-1} b_{\lfloor (i-1)/N_s \rfloor})$, where the data-modulated chip sequence $\{a_{i-L} b_{\lfloor (i-L)/N_s \rfloor}, \dots, a_{i-1} b_{\lfloor (i-1)/N_s \rfloor}\}$ corresponds to a path which takes the spreading "encoder" from a previous state σ_{i-L} to the present state σ_i . Note the combined trellis is also time varying with the period of N_s . The well-known Viterbi algorithm can be applied to the combined trellis, searching recursively for the maximum-likelihood sequence $\{b_n\}$.

Example 1: Consider a two-tap ISI channel ($L = 1$) with BPSK data symbols. The trellis for the spreading code with $N_s = 4$ is shown in Fig. 1. The combined trellis is shown in Fig. 2. We note the combined trellis has two states at any stage, with time-varying structure. Also note the label on the trellis transition is determined by the spreading sequence $\{a_i\}$ and the fading channel coefficients $\{z_l\}$. Applying the Viterbi algorithm, we only need to perform the addition-comparison-selection (ACS) operations at one stage in every N_s stages, and accumulate the path metrics for the remaining $N_s - 1$ stages.

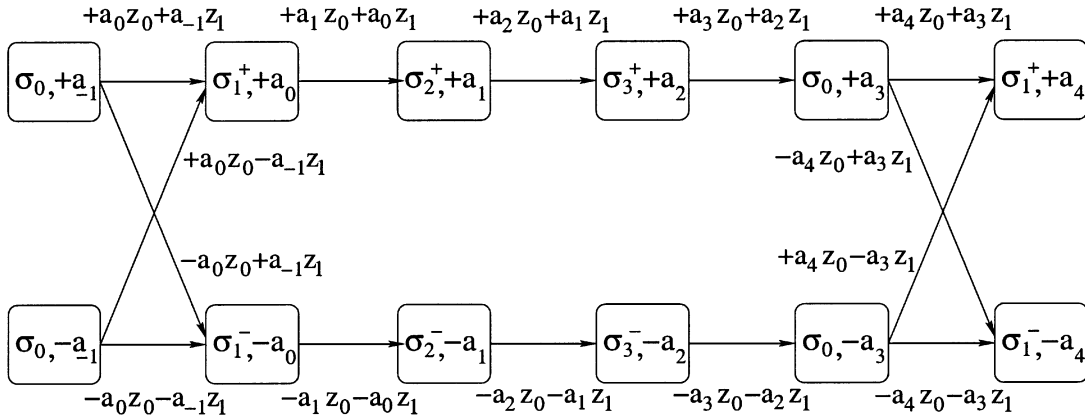


Fig. 2. Combined trellis of DSSS signal with BPSK data symbols on two-tap ISI channel, $N_s = 4$.

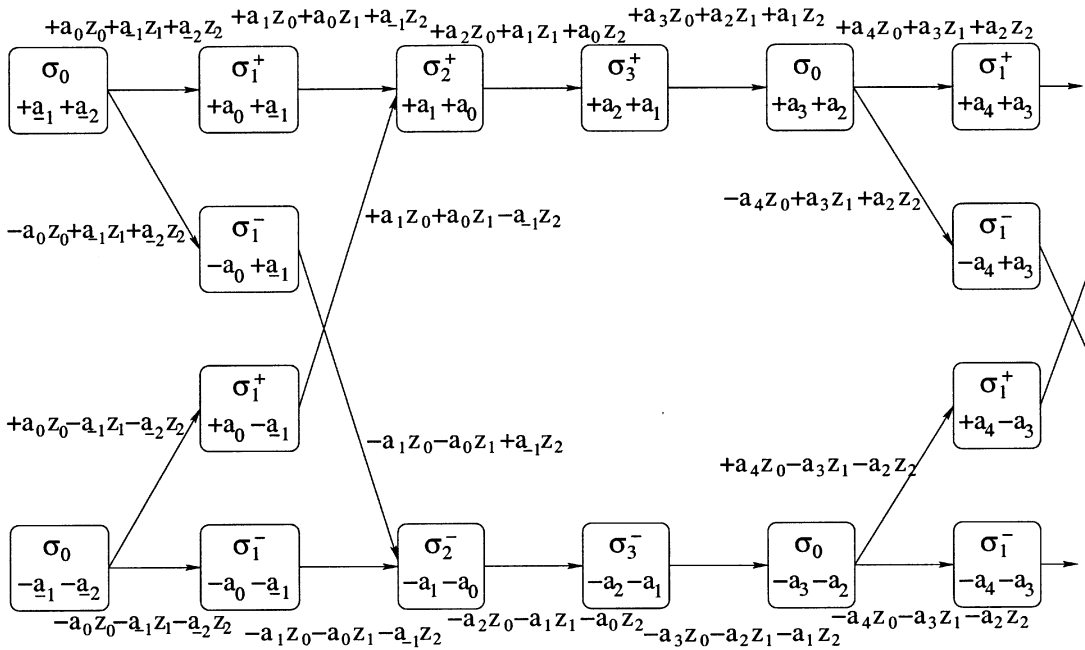


Fig. 3. Combined trellis of DSSS signal with BPSK data symbols on three-tap ISI channel, $N_s = 4$.

Example 2: Consider a three-tap ($L = 2$) ISI channel with BPSK data symbols. The combined trellis is shown in Fig. 3. Again, the combined trellis employs a time-varying structure, which repeats for every $N_s = 4$ trellis transition stages. For one stage out of every repeat period, when each of the two chips stored in the ISI channel memory are modulated by a distinct data bit, there are four states in the trellis. For all the other stages, there are only two states, since the two chips stored in the ISI channel memory are modulated by the same data bit.

The complexity of the proposed MLSE receiver increases with the processing gain, N_s , and the number of ISI channel taps. The maximal number of states per chip is $2^{\lceil(L-1)/N_s\rceil+1}$, while the number of transition branches per chip is either $2^{\lceil L/N_s \rceil+1}$ or $2^{\lceil L/N_s \rceil}$. The overall computational complexity of the MLSE receiver is dominated by the metric computations, which has complexity proportional to $N_s 2^{\lceil L/N_s \rceil}$. In other words, the complexity grows linearly with N_s , but exponentially with $\lceil L/N_s \rceil$. If $\lceil L/N_s \rceil$ is relatively small,

the complexity of the MLSE receiver will be acceptable, although the Viterbi algorithm has to run at the chip rate. As a comparison, the complexity of the conventional RAKE receiver is $N_s(L+1)$, which grows linearly with both N_s and L .

IV. PERFORMANCE ANALYSIS

A. Eigenanalysis Bound

We evaluate the bit-error probability of the MLSE receiver in a slow-fading Rayleigh channel, with the assumption that $\{z_i(t)\}$ remains constant over the length of the dominant error events. The standard union bound technique can be applied. Consider an error sequence $\boldsymbol{\varepsilon} = \mathbf{b} - \hat{\mathbf{b}}$ between the transmitted data vector \mathbf{b} and the detected data vector $\hat{\mathbf{b}}$, where $\varepsilon_n = 0, n < 0$ or $n \geq L_e$, and L_e is the length of the error event. The error sequence is simple, i.e., the transmitted path and detected path diverge at time 0 and remerge at time $(L_e N_s + L)T_c$, but do not

remerge at any time between them. The union bound is given by [8], [12]

$$P_b \leq \sum_{\boldsymbol{\varepsilon} \in \mathcal{E}} w(\boldsymbol{\varepsilon}) P_1(\boldsymbol{\varepsilon}) P_e(\boldsymbol{\varepsilon}) \quad (6)$$

where \mathcal{E} is the set of all simple error events starting at $n = 0$, $w(\boldsymbol{\varepsilon})$ is the number of bit errors associated with the error event $\boldsymbol{\varepsilon}$, $P_1(\boldsymbol{\varepsilon})$ is the probability that $\hat{\mathbf{b}} = \mathbf{b} - \boldsymbol{\varepsilon}$ is an allowable input sequence, and $P_e(\boldsymbol{\varepsilon})$ is the pairwise error probability that $\hat{\mathbf{b}}$ has a larger metric than the transmitted sequence \mathbf{b} . The pairwise error probability is represented by

$$P_e(\boldsymbol{\varepsilon}) = \Pr\{J(\hat{\mathbf{b}}) > J(\mathbf{b})\} \\ = \Pr\{\Delta J(\boldsymbol{\varepsilon}) < 0\} \quad (7)$$

where

$$\Delta J(\boldsymbol{\varepsilon}) = J(\mathbf{b}) - J(\hat{\mathbf{b}}) \\ = \sum_{i=0}^{L_\varepsilon N_s + L - 1} \left(2\Re \left\{ \eta_i^* \sum_{l=0}^L z_l a_{i-l} \varepsilon_{[i-l/N_s]} \right\} \right. \\ \left. + \left| \sum_{l=0}^L z_l a_{i-l} \varepsilon_{[i-l/N_s]} \right|^2 \right). \quad (8)$$

Conditioned on the channel vector $\mathbf{z} \triangleq [z_0, z_1, \dots, z_L]^T$, the pairwise error probability is given by [12]

$$P_e(\boldsymbol{\varepsilon}|\mathbf{z}) = Q \left(\sqrt{\frac{\Delta^2}{4\sigma_\eta^2}} \right) \quad (9)$$

where $Q(x) \triangleq (1/\sqrt{2\pi}) \int_x^\infty e^{-t^2/2} dt$, and Δ^2 is the squared Euclidean path distance, given by [10]

$$\Delta^2 = \sum_{i=0}^{L_\varepsilon N_s + L - 1} \left| \sum_{l=0}^L z_l a_{i-l} \varepsilon_{[i-l/N_s]} \right|^2 \\ \triangleq \mathbf{z}^H E \mathbf{z}. \quad (10)$$

Here, the path distance matrix $E \triangleq \sum_{i=0}^{L_\varepsilon N_s + L - 1} E(i)$, and $E(i) = \mathbf{e}_i \mathbf{e}_i^H$, where the error vector \mathbf{e}_i is defined as $[a_i \varepsilon_{[i/N_s]}, a_{i-1} \varepsilon_{[i-1/N_s]}, \dots, a_{i-L} \varepsilon_{[i-L/N_s]}]^H$.

Assuming independence between the fading coefficients, z_l , of different paths, the pairwise error probability can be obtained in a closed form. Define the normalized channel vector $\mathbf{g} = [g_0, g_1, \dots, g_L]^T$, where $g_l = z_l/\Omega_l$. Equation (10) can be written as [14]

$$\Delta^2 = \mathbf{g}^H F \mathbf{g} \quad (11)$$

where

$$F = \boldsymbol{\Omega}^H E \boldsymbol{\Omega}. \quad (12)$$

Averaging over the normalized channel vector \mathbf{g} , the pairwise error probability is shown in [14] to be

$$P_e(\boldsymbol{\varepsilon}) = \frac{1}{2} \sum_{l=0}^L A_l (1 - \mu_l) \quad (13)$$

where

$$\mu_l = \sqrt{\frac{\lambda_l}{\lambda_l + 8\sigma_\eta^2}} \quad (14)$$

$$A_l = \prod_{i \neq l} \frac{\lambda_l}{\lambda_l - \lambda_i} \quad (15)$$

and $\{\lambda_l\}$ are eigenvalues of the matrix F , which are assumed to be distinct.

The union bound in (6) requires the calculation of an infinite series. In practice, the series needs to be truncated at an appropriate point. In addition, since the $(L+1) \times (L+1)$ matrix E is determined by both the error sequence $\boldsymbol{\varepsilon}$, and the random spreading sequence $\{a_i\}$, the randomness of E has to be taken into consideration. The analysis is illustrated in the examples in Section V.

B. Numerical Bound

The bound in the last subsection is analytically tractable, and provides useful insights into the system. However, the results from the bound may be loose [10]. Due to the lack of time diversity, the probability of longer error events does not diminish as fast as on a fast-fading channel, and there is no dominant error event for the slow-fading channel. The approach considered in this subsection limits the conditional bit-error probability before averaging over the channel vector \mathbf{z} [15]. This approach does not involve the truncation of the sum over the simple error events, and may yield tighter results. The disadvantage of this method is that numerical integrations are required.

Assuming the channel vector \mathbf{z} is fixed, the conditional bit-error probability can be bounded using the transfer function of the error-state diagram [11]. Let $T(W, I)$ be the transfer function given by $T(W, I) = \sum t_{\Delta^2, i} W^{\Delta^2} I^i$, where $t_{\Delta^2, i}$ is the number of error events that have squared Euclidean distance Δ^2 and i data bit errors. Then the Bhattacharyya bound can be used for the conditional bit-error probability [16]

$$P_b(\mathbf{z}) \leq Q \left(\sqrt{\frac{d_f^2 E_s}{2N_0}} \right) \exp \left(\frac{d_f^2 E_s}{4N_0} \right) \\ \frac{\partial T}{\partial I} \left(W = \exp \left(-\frac{E_s}{4N_0} \right), I = 1 \right) \quad (16)$$

where d_f^2 is the minimal squared Euclidean distance.

We can also use an alternate form of the Gaussian Q -function [17] to evaluate the exact transfer function bound on the bit-error probability conditioned on the fading channel, as demonstrated in Appendix II. Note the transfer function $T(W, I)$ is dependent on the channel vector \mathbf{z} . A tight bound is obtained by limiting the conditional union bound below $1/2$ before averaging over the channel vector [15], yielding

$$P_b \leq \int_{\mathbf{z}} \min \left[\frac{1}{2}, P_b(\mathbf{z}) \right] f(\mathbf{z}) d\mathbf{z} \quad (17)$$

where $f(\mathbf{z})$ is the probability density function of the channel vector. Due to the minimization, the integration has to be carried out numerically.

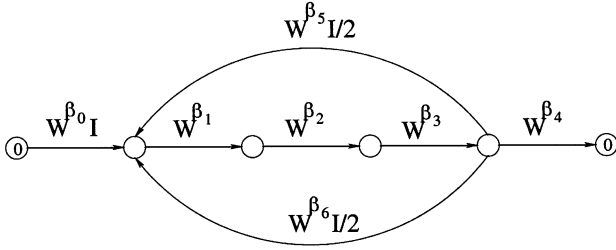


Fig. 4. Reduced error-state diagram of DSSS signal with BPSK data symbols on two-tap ISI channel, $N_s = 4$.

TABLE I

ELEMENTS OF BRANCH DISTANCE MATRIX E_j FOR BPSK SYMBOLS OVER A TWO-TAP ISI CHANNEL, ASSUMING $N_s = 4$. NOTE FOR A SHORT SPREADING SEQUENCE, $a_4 = a_0$

	(1, 1)	(1, 2)	(2, 2)
$E_0/4$	$ a_0 ^2$	0	0
$E_1/4$	$ a_1 ^2$	$a_0 a_1^*$	$ a_0 ^2$
$E_2/4$	$ a_2 ^2$	$a_1 a_2^*$	$ a_1 ^2$
$E_3/4$	$ a_3 ^2$	$a_2 a_3^*$	$ a_2 ^2$
$E_4/4$	0	0	$ a_3 ^2$
$E_5/4$	$ a_4 ^2$	$a_3 a_4^*$	$ a_3 ^2$
$E_6/4$	$ a_4 ^2$	$-a_3 a_4^*$	$ a_3 ^2$

V. EXAMPLES AND DISCUSSION

A. BPSK Data Symbols on a Two-Tap ISI Channel

We revisit *Example 1* from Section III. This is an ISI channel with one interfering symbol, and the combined trellis is shown in Fig. 2. Following the steps of the analysis on ISI channels in [11], the reduced error-state diagram for a short spreading sequence with $N_s = 4$ is obtained and shown in Fig. 4. The squared Euclidean distance and the number of data bit errors associated with each branch are represented as the exponents of W and I . The squared Euclidean distance, $\beta_j, j = 0, \dots, 6$, are represented in the following as quadratic forms in the channel vector \mathbf{z} , where the branch distance matrices associated with the quadratic form, $E_j, j = 0, \dots, 6$, are shown in Table I. Since the matrices are Hermitian, only the upper triangular elements are listed.

$$\begin{aligned}\beta_0 &= 4|a_0 z_0|^2 = \mathbf{z}^H E_0 \mathbf{z} \\ \beta_1 &= 4|a_1 z_0 + a_0 z_1|^2 = \mathbf{z}^H E_1 \mathbf{z} \\ \beta_2 &= 4|a_2 z_0 + a_1 z_1|^2 = \mathbf{z}^H E_2 \mathbf{z} \\ \beta_3 &= 4|a_3 z_0 + a_2 z_1|^2 = \mathbf{z}^H E_3 \mathbf{z} \\ \beta_4 &= 4|a_3 z_1|^2 = \mathbf{z}^H E_4 \mathbf{z} \\ \beta_5 &= 4|a_4 z_0 + a_3 z_1|^2 = \mathbf{z}^H E_5 \mathbf{z} \\ \beta_6 &= 4|a_4 z_0 - a_3 z_1|^2 = \mathbf{z}^H E_6 \mathbf{z}.\end{aligned}$$

With the help of the error-state diagram, we can obtain the path distance matrix E , the squared Euclidean distance $\Delta^2 = \mathbf{z}^H E \mathbf{z}$, and the associated probability $P_1(\boldsymbol{\varepsilon})$, for any simple error sequence. Consider an error event with w information bit errors. From Fig. 4, we know it passes through the feedback branches (β_5 or β_6) $w - 1$ times. The enumerating function of

the squared Euclidean distances is

$$\begin{aligned}W^{\beta_0 + \beta_1 + \beta_2 + \beta_3 + \beta_4} \left[\frac{1}{2} (W^{\beta_5} + W^{\beta_6}) W^{\beta_1 + \beta_2 + \beta_3} \right]^{w-1} \\ = \sum_{p=0}^{w-1} \binom{w-1}{p} 2^{1-w} W^{p\beta_6 + (w-1-p)\beta_5 + w(\beta_1 + \beta_2 + \beta_3) + \beta_0 + \beta_4}\end{aligned}\quad (18)$$

where p is the number of times the error event takes β_6 as its feedback branch. Since $\beta_j = \mathbf{z}^H E_j \mathbf{z}, j = 0, \dots, 6$, the path distance matrix of the error event with w bit errors and a specified value of p , denoted by $E(w, p)$, is given by

$$\begin{aligned}E(w, p) &= pE_6 + (w-1-p)E_5 \\ &\quad + w(E_1 + E_2 + E_3) + E_0 + E_4 \\ &= 4 \begin{bmatrix} wN_s & U(w, p) \\ U^*(w, p) & wN_s \end{bmatrix}\end{aligned}\quad (19)$$

where $U(w, p) = wC(1) + (w-1-2p)a_{N_s-1}a_0^*$, and $C(1) = \sum_{i=0}^{N_s-2} a_i a_{i+1}^*$ is the discrete aperiodic autocorrelation function of the short spreading sequence \mathbf{a} , with an offset one [18]. The probability $P_1(\boldsymbol{\varepsilon})$ associated with the error event, denoted by $P_1(w, p)$, is

$$P_1(w, p) = \binom{w-1}{p} 2^{1-w}.\quad (20)$$

To obtain a similar result for a random spreading sequence, we need a vector $\mathbf{p} = [p_1, p_2, \dots, p_{w-1}]^T$ to record the choice of the feedback branches in order. The sequence $\{p_n\}_{n=1}^{w-1}$ is defined as

$$p_n \triangleq \begin{cases} +1, & \text{if } \beta_5 \text{ is chosen} \\ -1, & \text{if } \beta_6 \text{ is chosen.} \end{cases}\quad (21)$$

The path distance matrix of the error event with w bit errors and a specified vector \mathbf{p} , denoted by $E(w, \mathbf{p})$, is expressed as

$$E(w, \mathbf{p}) = 4 \begin{bmatrix} wN_s & U(w, \mathbf{p}) \\ U(w, \mathbf{p}) & wN_s \end{bmatrix}\quad (22)$$

where

$$U(w, \mathbf{p}) = \sum_{\substack{i=0 \\ (i+1) \bmod N_s \neq 0}}^{wN_s-2} a_i a_{i+1}^* + \sum_{n=1}^{w-1} p_n a_{nN_s-1} a_{nN_s}^*$$

and the associated probability of the error event is $P_1(w, \mathbf{p}) = 2^{1-w}$.

Next, the randomness of the spreading sequence $\{a_i\}$ is taken into consideration. A new sequence of binary random variables, $\{c_i\}$, is defined by

$$c_i = \begin{cases} a_i a_{i+1}^*, & \text{if } (i+1) \bmod N_s \neq 0 \\ p_n a_{nN_s-1} a_{nN_s}^*, & \text{if } i = nN_s - 1. \end{cases}\quad (23)$$

Since $\{a_i\}$ is a sequence of i.i.d. binary random variables on $\{\pm 1\}$, $\{c_i\}$ is also a sequence of i.i.d. random variables on $\{\pm 1\}$. The random variable $U(w, \mathbf{p})$ can be written as

$$U(w, \mathbf{p}) = \sum_{i=0}^{wN_s-2} c_i.\quad (24)$$

The path distance matrix $E(w, \mathbf{p})$ is fully determined by w and U through (22), and is denoted by $E(w, U)$. Correspondingly, the associated probability P_1 is also determined by w and U via

$$P_1(w, U) = \binom{wN_s - 1}{m} 2^{1-wN_s} \quad (25)$$

$$m = 0, 1, \dots, wN_s - 1$$

where $m = (wN_s - 1 - U/2)$ denotes the number of c_i 's in the sum of (24) that take the value of “-1”.

Now (6)–(15) can be applied to obtain the union bound on the bit-error probability. For the special case of flat MIP, i.e., $\mathbf{\Omega} = \text{diag}\{1/\sqrt{2}, 1/\sqrt{2}\}$, we have

$$F(w, U) = \mathbf{\Omega}^H E(w, U) \mathbf{\Omega} = \frac{1}{2} E(w, U). \quad (26)$$

The eigenvalues of $F(w, U)$ are

$$\lambda_1 = 2(wN_s + |U|)$$

$$\lambda_2 = 2(wN_s - |U|).$$

If N_s is an even number, we have $U \neq 0$ and $\lambda_1 \neq \lambda_2$. The pairwise error probability is given by

$$P_e(w, U) = \frac{1}{2} [A_1(1 - \mu_1) + A_2(1 - \mu_2)]$$

$$A_1 = \frac{1}{2} + \frac{wN_s}{2|U|}$$

$$A_2 = \frac{1}{2} - \frac{wN_s}{2|U|}$$

where μ_1 and μ_2 are given by (14). The union bound on the bit-error probability is given by

$$P_b \leq \sum_{w=1}^{\infty} \sum_{m=0}^{wN_s-1} w \binom{wN_s - 1}{m} 2^{1-wN_s} \times P_e(w, wN_s - 1 - 2m). \quad (27)$$

Alternatively, the numerical bound can be applied to estimate the bit-error probability. Conditioned on the channel vector $\{z_l = \alpha_l e^{j\psi_l}\}$, the labels on the branches of the error-state diagram (Fig. 4) are given by

$$\beta_0 = 4\alpha_0^2$$

$$\beta_1 = 4(\alpha_0^2 + 2a_0a_1\alpha_0\alpha_1 \cos \theta + \alpha_1^2)$$

$$\beta_2 = 4(\alpha_0^2 + 2a_1a_2\alpha_0\alpha_1 \cos \theta + \alpha_1^2)$$

$$\beta_3 = 4(\alpha_0^2 + 2a_2a_3\alpha_0\alpha_1 \cos \theta + \alpha_1^2)$$

$$\beta_4 = 4\alpha_1^2$$

$$\beta_5 = 4(\alpha_0^2 + 2a_3a_4\alpha_0\alpha_1 \cos \theta + \alpha_1^2)$$

$$\beta_6 = 4(\alpha_0^2 - 2a_3a_4\alpha_0\alpha_1 \cos \theta + \alpha_1^2)$$

where $\theta = \psi_1 - \psi_0$ is the relative phase.

Note $\{a_i a_{i+1}\}$ are independent random variables taking ± 1 with equal probability of 1/2. This randomness can be reflected in the error-state diagram by splitting the branches of $\beta_i, i = 1, 2, 3, 5, 6$. In addition, the four branches obtained by splitting the branches β_5 and β_6 can be merged into two. The modified

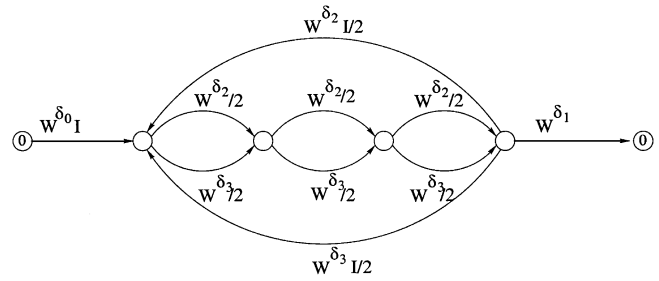


Fig. 5. Modified error-state diagram taking the randomness of the spreading sequence into account, BPSK data symbols on two-tap ISI channel. $N_s = 4$.

error-state diagram is depicted in Fig. 5, with the labels defined by

$$\delta_0 = 4\alpha_0^2$$

$$\delta_1 = 4\alpha_1^2$$

$$\delta_2 = 4(\alpha_0^2 + 2\alpha_0\alpha_1 \cos \theta + \alpha_1^2)$$

$$\delta_3 = 4(\alpha_0^2 - 2\alpha_0\alpha_1 \cos \theta + \alpha_1^2).$$

By symmetry, the relative phase θ can be treated as a random variable uniformly distributed in the range of $[0, \pi/2]$. The transfer function of this diagram can be shown to be

$$T(W, I) = \frac{B^{N_s-1}(W)W^{\delta_0+\delta_1}I}{1 - B^{N_s}(W)I} \quad (28)$$

$$\frac{\partial T}{\partial I}(W, I)|_{I=1} = \frac{B^{N_s-1}(W)W^{\delta_0+\delta_1}}{[1 - B^{N_s}(W)]^2} \quad (29)$$

where

$$B(W) \triangleq \frac{1}{2}(W^{\delta_2} + W^{\delta_3}). \quad (30)$$

Using (16), the conditional bit-error probability is upper bounded by

$$P_b(\alpha_0, \alpha_1, \theta) \leq Q\left(\sqrt{\frac{d_f^2 E_s}{2N_0}}\right) e^{(N_s-1)\delta_3(E_s/4N_0)} \frac{B^{N_s-1}(e^{-(E_s/4N_0)})}{(1 - B^{N_s}(e^{-(E_s/4N_0)}))^2} \quad (31)$$

where

$$d_f^2 = \delta_0 + \delta_1 + (N_s - 1)\delta_3. \quad (32)$$

Finally, the bit-error probability is upper bounded by

$$P_b \leq \int_{\alpha_0=0}^{\infty} \int_{\alpha_1=0}^{\infty} \int_{\theta=0}^{\pi/2} \min\left[\frac{1}{2}, P_b(\alpha_0, \alpha_1, \theta)\right] \times f_{\alpha_0}(\alpha_0) f_{\alpha_1}(\alpha_1) f_{\theta}(\theta) d\theta d\alpha_1 d\alpha_0 \quad (33)$$

where $f_{\alpha_i}(\alpha_i)$ and $f_{\theta}(\theta)$ are the probability density functions of the Rayleigh fading amplitudes, α_i , and the relative phase θ , respectively.

In Fig. 6, the two upper bounds on the bit-error probability are shown, together with the simulation results for the two-tap ISI channel. The eigenanalysis bounds are shown with the infinite sum over w truncated at different values ($w_{\max} = 5, 25$, or

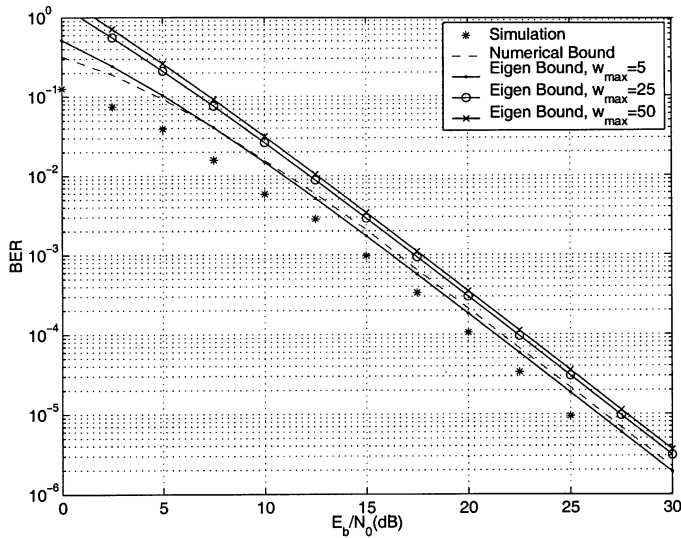


Fig. 6. Comparison of the analytical bounds and simulation results for MLSE receiver for DS-BPSK signal, two-tap ISI channel, random spreading sequence, $N_s = 4$.

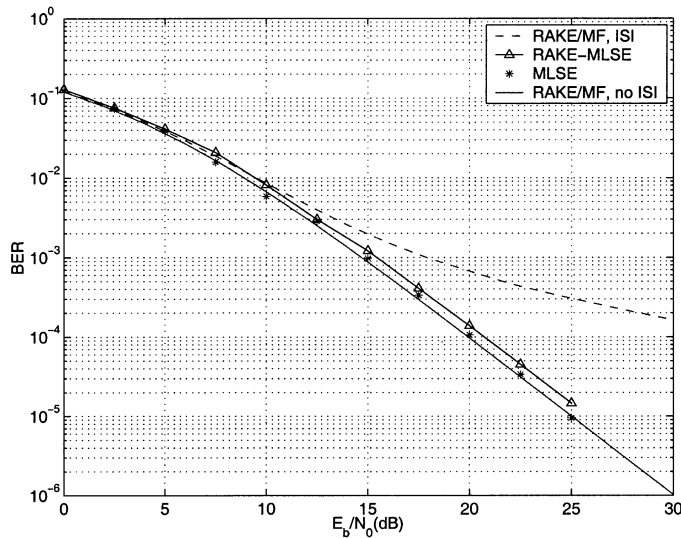


Fig. 7. Comparison of the performance of MLSE receiver with the conventional RAKE receiver (with or without ISI) and the RAKE-MLSE receiver, DS-BPSK signal, two-tap ISI channel, random spreading sequence, $N_s = 4$.

50). Since the results do not change much when increasing the w_{\max} from 25 to 50, $w_{\max} = 25$ seems to be sufficient for computing the eigenanalysis bound. The bound based on numerical integration is tighter than the eigenanalysis bound, especially at low E_b/N_0 values, and it is within 2 dB of the simulation results.

In Fig. 7, the performance of the MLSE receiver is compared to that of the conventional RAKE receiver, both with and without ISI. The bit-error rate (BER) curves for the conventional RAKE receiver are generated by using the characteristic function method [19], with a sample average over 1000 realizations of the random spreading sequences. The performance of the RAKE-MLSE receiver in [5], obtained from simulation, is also shown in the figure. It can be seen that while ISI introduces an error floor for the conventional RAKE receiver, the MLSE

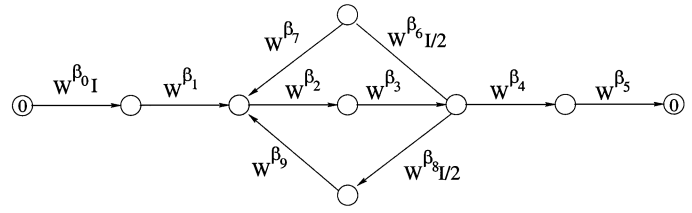


Fig. 8. Reduced error-state diagram of DSSS signal with BPSK data symbols on three-tap ISI channel, $N_s = 4$.

TABLE II
ELEMENTS OF BRANCH DISTANCE MATRIX E_j FOR BPSK SYMBOLS OVER A THREE-TAP ISI CHANNEL, ASSUMING $N_s = 4$. NOTE FOR A SHORT SPREADING SEQUENCE, $a_4 = a_0$, $a_5 = a_1$

	(1, 1)	(1, 2)	(1, 3)	(2, 2)	(2, 3)	(3, 3)
$E_0/4$	$ a_0 ^2$	0	0	0	0	0
$E_1/4$	$ a_1 ^2$	$a_0 a_1^*$	0	$ a_0 ^2$	0	0
$E_2/4$	$ a_2 ^2$	$a_1 a_2^*$	$a_0 a_2^*$	$ a_1 ^2$	$a_0 a_1^*$	$ a_0 ^2$
$E_3/4$	$ a_3 ^2$	$a_2 a_3^*$	$a_1 a_3^*$	$ a_2 ^2$	$a_1 a_2^*$	$ a_1 ^2$
$E_4/4$	0	0	0	$ a_3 ^2$	$a_2 a_3^*$	$ a_2 ^2$
$E_5/4$	0	0	0	0	0	$ a_3 ^2$
$E_6/4$	$ a_4 ^2$	$a_3 a_4^*$	$a_2 a_4^*$	$ a_3 ^2$	$a_2 a_3^*$	$ a_2 ^2$
$E_7/4$	$ a_5 ^2$	$a_4 a_5^*$	$a_3 a_5^*$	$ a_4 ^2$	$a_3 a_4^*$	$ a_3 ^2$
$E_8/4$	$ a_4 ^2$	$-a_3 a_4^*$	$-a_2 a_4^*$	$ a_3 ^2$	$a_2 a_3^*$	$ a_2 ^2$
$E_9/4$	$ a_5 ^2$	$a_4 a_5^*$	$-a_3 a_5^*$	$ a_4 ^2$	$-a_3 a_4^*$	$ a_3 ^2$

receiver can recover almost all the loss due to ISI. In addition, it is found that the proposed MLSE receiver outperforms the RAKE-MLSE receiver by a small margin.

B. BPSK Data Symbols on a Three-Tap ISI Channel

Both the analytical bounds can be extended to BPSK data symbols on a three-tap ISI channel. The combined trellis is illustrated in Fig. 3. The reduced error-state diagram for a short spreading sequence with $N_s = 4$ is shown in Fig. 8. Note the branches β_2 and β_3 correspond to the transitions from state σ_2 to σ_3 , and from state σ_3 to σ_4 in Fig. 3, respectively. The squared Euclidean distances on each branch are given below. The matrix E_j is shown in Table II. Since the matrix E_j 's are Hermitian, only the upper triangular elements are listed.

$$\begin{aligned}
 \beta_0 &= 4|a_0 z_0|^2 = \mathbf{z}^H E_0 \mathbf{z} \\
 \beta_1 &= 4|a_1 z_0 + a_0 z_1|^2 = \mathbf{z}^H E_1 \mathbf{z} \\
 \beta_2 &= 4|a_2 z_0 + a_1 z_1 + a_0 z_2|^2 = \mathbf{z}^H E_2 \mathbf{z} \\
 \beta_3 &= 4|a_3 z_0 + a_2 z_1 + a_1 z_2|^2 = \mathbf{z}^H E_3 \mathbf{z} \\
 \beta_4 &= 4|a_3 z_1 + a_2 z_2|^2 = \mathbf{z}^H E_4 \mathbf{z} \\
 \beta_5 &= 4|a_3 z_2|^2 = \mathbf{z}^H E_5 \mathbf{z} \\
 \beta_6 &= 4|a_4 z_0 + a_3 z_1 + a_2 z_2|^2 = \mathbf{z}^H E_6 \mathbf{z} \\
 \beta_7 &= 4|a_5 z_0 + a_4 z_1 + a_3 z_2|^2 = \mathbf{z}^H E_7 \mathbf{z} \\
 \beta_8 &= 4|a_4 z_0 - a_3 z_1 - a_2 z_2|^2 = \mathbf{z}^H E_8 \mathbf{z} \\
 \beta_9 &= 4|a_5 z_0 + a_4 z_1 - a_3 z_2|^2 = \mathbf{z}^H E_9 \mathbf{z}.
 \end{aligned}$$

Similar to the two-tap ISI channel, we can obtain the path distance matrix E and the associated probability $P_1(\epsilon)$ for any simple error sequence. An error event with w information bit errors has to pass the feedback branches (β_6/β_7 or β_8/β_9) $w-1$

times. Let p denotes the number of times the error event takes β_8/β_9 as its feedback branches. Then the path matrix is given by

$$E(w, p) = 4 \begin{bmatrix} wN_s & U_1(w, p) & U_2(w, p) \\ U_1^*(w, p) & wN_s & U_1(w, p) \\ U_2^*(w, p) & U_1^H(w, p) & wN_s \end{bmatrix}$$

where

$$\begin{aligned} U_1(w, p) &= wC(1) + (w - 1 - 2p)a_{N_s-1}a_0^* \\ U_2(w, p) &= wC(2) + (w - 1 - 2p)(a_{N_s-2}a_0^* + a_{N_s-1}a_1^*). \end{aligned}$$

Again, $C(1)$ and $C(2)$ are the discrete aperiodic autocorrelation function of the short spreading sequence, with offset one and two, respectively, and the associated probability is the same as that given in (20).

For random spreading sequence, we also define a vector \mathbf{p} to record the choice of the feedback branches in order

$$p_n \triangleq \begin{cases} +1, & \text{if } \beta_6/\beta_7 \text{ is chosen} \\ -1, & \text{if } \beta_8/\beta_9 \text{ is chosen} \end{cases} \quad n = 1, 2, \dots, w-1. \quad (34)$$

The path distance matrix is expressed by

$$E(w, \mathbf{p}) = 4 \begin{bmatrix} wN_s & U_1(w, \mathbf{p}) & U_2(w, \mathbf{p}) \\ U_1^*(w, \mathbf{p}) & wN_s & U_1(w, \mathbf{p}) \\ U_2^*(w, \mathbf{p}) & U_1^*(w, \mathbf{p}) & wN_s \end{bmatrix} \quad (35)$$

where

$$\begin{aligned} U_1(w, \mathbf{p}) &\triangleq \sum_{\substack{i=0 \\ (i+1) \bmod N_s \neq 0}}^{wN_s-2} a_i a_{i+1}^* + \sum_{n=1}^{w-1} p_n a_{nN_s-1} a_{nN_s}^* \\ U_2(w, \mathbf{p}) &\triangleq \sum_{\substack{i=0 \\ (i+2) \bmod N_s \neq 0, 1}}^{wN_s-3} a_i a_{i+2}^* \\ &\quad + \sum_{n=1}^{w-1} p_n (a_{nN_s-2} a_{nN_s}^* + a_{nN_s-1} a_{nN_s+1}^*) \end{aligned}$$

and the associated probability is $P_1(w, \mathbf{p}) = 2^{1-w}$.

Defining a new sequence of i.i.d. binary random variables $\{c_i\}$ as in (23), we have

$$\begin{aligned} U_1(w, \mathbf{p}) &= \sum_{i=0}^{wN_s-2} c_i \\ U_2(w, \mathbf{p}) &= \sum_{i=0}^{wN_s-3} c_i c_{i+1}. \end{aligned}$$

The path distance matrix $E(w, \mathbf{p})$ is fully determined by w , U_1 , and U_2 . For a given value of w , U_1 and U_2 are functions of the i.i.d. binary random variables $\{c_i\}$, and their joint density function is determined as follows. Let m_1 and m_2 be the number of “-1” terms in the summation of U_1 and U_2 , respectively. Equivalently

$$\begin{aligned} U_1 &= wN_s - 1 - 2m_1 \\ U_2 &= wN_s - 2 - 2m_2. \end{aligned}$$

Note the sequences $\{c_i\}$ and $\{c_i c_{i+1}\}$ can be considered as the input and output sequence of a $1+D$ encoder. Correspondingly, m_1 and m_2 is the input and output weight of the encoder, respectively. In Appendix I, we derive the joint input-output weight enumerating function (IOWEF) of the $1+D$ encoder. Letting $A_{w,h}$ represent the number of codewords with output weight h generated by input words of weight w , the associated probability with w, m_1, m_2 is given by

$$P_1(w, m_1, m_2) = A_{m_1, m_2} 2^{1-wN_s}. \quad (36)$$

The union bound on the bit-error probability is given by

$$P_b \leq \sum_{w=1}^{\infty} \sum_{m_1=0}^{wN_s-1} \sum_{m_2=0}^{wN_s-2} w A_{m_1, m_2} 2^{1-wN_s} P_e(w, U_1, U_2) \quad (37)$$

where $P_e(w, U_1, U_2)$ is the pairwise error probability determined by (12)–(15), with the matrix E given in (35).

The numerical bound can also be applied for the three-tap ISI channel. Given the channel vector $\{z_l = \alpha_l e^{j\psi_l}\}_{l=0}^2$, define the relative phases $\theta_1 = \psi_1 - \psi_0$ and $\theta_2 = \psi_2 - \psi_0$, which can be modeled as two independent random variables uniformly distributed in $[0, \pi]$. By using the definition of $\{c_i\}$ in (23) with p_n defined in (34), the labels on the branches of the error-state diagram (Fig. 8) can be written as

$$\begin{aligned} \beta_0 &= 4\alpha_0^2 \\ \beta_1 &= 4(\alpha_0^2 + \alpha_1^2 + 2c_0\alpha_0\alpha_1 \cos \theta_1) \\ \beta_2 &= 4(\alpha_0^2 + \alpha_1^2 + \alpha_2^2 + 2c_1\alpha_0\alpha_1 \cos \theta_1 \\ &\quad + 2c_0\alpha_1\alpha_2 \cos \theta_2 + 2c_0c_1\alpha_0\alpha_1 \cos(\theta_2 - \theta_1)) \\ \beta_3 &= 4(\alpha_0^2 + \alpha_1^2 + \alpha_2^2 + 2c_2\alpha_0\alpha_1 \cos \theta_1 \\ &\quad + 2c_1\alpha_1\alpha_2 \cos \theta_2 + 2c_1c_2\alpha_0\alpha_1 \cos(\theta_2 - \theta_1)) \\ \beta_4 &= 4(\alpha_1^2 + \alpha_2^2 + 2c_2\alpha_1\alpha_2 \cos \theta_2) \\ \beta_5 &= 4\alpha_2^2 \\ \beta_6 &= 4(\alpha_0^2 + \alpha_1^2 + \alpha_2^2 + 2c_3\alpha_0\alpha_1 \cos \theta_1 \\ &\quad + 2c_2\alpha_1\alpha_2 \cos \theta_2 + 2c_2c_3\alpha_0\alpha_1 \cos(\theta_2 - \theta_1)) \\ \beta_7 &= 4(\alpha_0^2 + \alpha_1^2 + \alpha_2^2 + 2c_4\alpha_0\alpha_1 \cos \theta_1 \\ &\quad + 2c_3\alpha_1\alpha_2 \cos \theta_2 + 2c_3c_4\alpha_0\alpha_1 \cos(\theta_2 - \theta_1)) \\ \beta_8 &= 4(\alpha_0^2 + \alpha_1^2 + \alpha_2^2 + 2c_3\alpha_0\alpha_1 \cos \theta_1 \\ &\quad + 2c_2\alpha_1\alpha_2 \cos \theta_2 + 2c_2c_3\alpha_0\alpha_1 \cos(\theta_2 - \theta_1)) \\ \beta_9 &= 4(\alpha_0^2 + \alpha_1^2 + \alpha_2^2 + 2c_4\alpha_0\alpha_1 \cos \theta_1 \\ &\quad + 2c_3\alpha_1\alpha_2 \cos \theta_2 + 2c_3c_4\alpha_0\alpha_1 \cos(\theta_2 - \theta_1)). \end{aligned}$$

Note the labels β_8 and β_9 are the same as the labels β_6 and β_7 , respectively, because the difference in sign has been absorbed into the random variable c_i . The error-state diagram can be modified to take into account the randomness of c_i . For example, the branch of β_1 is split for two possible values of c_0 . Conditioned on c_0 (which becomes the state in the error-state diagram), the branch of β_2 can take two possible values, according to c_1 . Thus, states between the branches are introduced in the diagram. The modified error-state diagram, which depicts a trellis structure, is shown in Fig. 9. Note that the exponentials of W of the branches connecting nonzero states are denoted as $\rho_{\sigma_s \sigma_e}$, where σ_s and σ_e are the symbols (“1”, “+”, “-”, or “2”) of the starting and

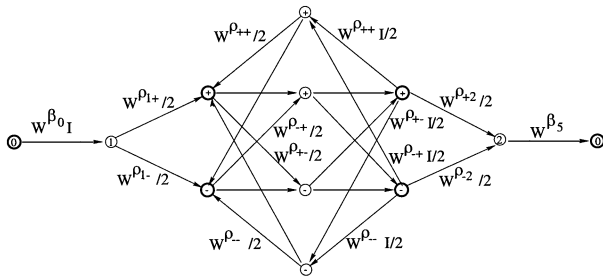


Fig. 9. Modified error-state diagram taking the randomness of the spreading sequence into account, BPSK data symbols on three-tap ISI channel, $N_s = 4$.

ending states of the branches, respectively. The branch labels in the diagram are defined as

$$\begin{aligned} \rho_{1+} &= 4(\alpha_0^2 + \alpha_1^2 + 2\alpha_0\alpha_1 \cos \theta_1) \\ \rho_{1-} &= 4(\alpha_0^2 + \alpha_1^2 - 2\alpha_0\alpha_1 \cos \theta_1) \\ \rho_{++} &= 4(\alpha_0^2 + \alpha_1^2 + \alpha_2^2 + 2\alpha_0\alpha_1 \cos \theta_1 \\ &\quad + 2\alpha_1\alpha_2 \cos \theta_2 + 2\alpha_0\alpha_2 \cos(\theta_2 - \theta_1)) \\ \rho_{+-} &= 4(\alpha_0^2 + \alpha_1^2 + \alpha_2^2 - 2\alpha_0\alpha_1 \cos \theta_1 \\ &\quad + 2\alpha_1\alpha_2 \cos \theta_2 - 2\alpha_0\alpha_2 \cos(\theta_2 - \theta_1)) \\ \rho_{-+} &= 4(\alpha_0^2 + \alpha_1^2 + \alpha_2^2 + 2\alpha_0\alpha_1 \cos \theta_1 \\ &\quad - 2\alpha_1\alpha_2 \cos \theta_2 - 2\alpha_0\alpha_2 \cos(\theta_2 - \theta_1)) \\ \rho_{--} &= 4(\alpha_0^2 + \alpha_1^2 + \alpha_2^2 - 2\alpha_0\alpha_1 \cos \theta_1 \\ &\quad - 2\alpha_1\alpha_2 \cos \theta_2 + 2\alpha_0\alpha_2 \cos(\theta_2 - \theta_1)) \\ \rho_{+2} &= 4(\alpha_1^2 + \alpha_2^2 + 2\alpha_1\alpha_2 \cos \theta_2) \\ \rho_{-2} &= 4(\alpha_1^2 + \alpha_2^2 - 2\alpha_1\alpha_2 \cos \theta_2). \end{aligned}$$

The transfer function can be found for the modified error-state diagram. The upper bound on the conditional bit-error probability $P_b(\alpha_0, \alpha_1, \alpha_2, \theta_1, \theta_2)$ is obtained in Appendix II. Finally, the bit-error probability is upper bounded by the equation shown at the bottom of the page, where $f_{\alpha_i}(\alpha_i)$ and $f_{\theta_i}(\theta_i)$ are the probability density functions of the Rayleigh fading amplitudes, α_i , and the relative phases, θ_i , respectively.

In Fig. 10, the two upper bounds on the bit-error probability are compared with the simulation results for the three-tap ISI channel. The eigenanalysis bound results remain virtually the same when increasing w_{\max} from 15 to 50, suggesting that $w_{\max} = 15$ is sufficient for computing the eigenanalysis bound. The bound based on numerical integration falls almost on top of the eigenanalysis bound; though it is tighter at very low E_b/N_0 values, since it performs the truncation before averaging. The bounds are within 1 dB of the simulation results, tighter than on the two-tap ISI channel.

In Fig. 11, the performance of the MLSE receiver is compared with that of the conventional RAKE receiver and simulation results of the RAKE-MLSE receiver in [5]. Comparing with the analytical results of the RAKE receiver, we observe that the error floor introduced by the ISI is higher than in the two-tap

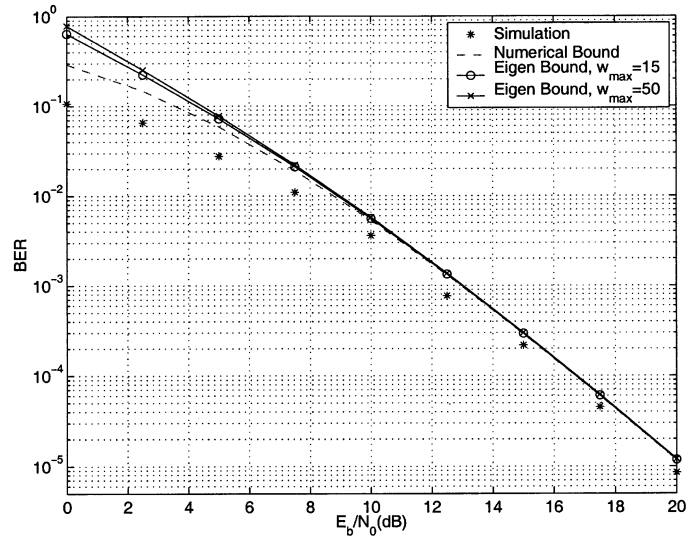


Fig. 10. Comparison of the analytical bounds and simulation results for MLSE receiver for DS-BPSK signal, three-tap ISI channel, random spreading sequence, $N_s = 4$.

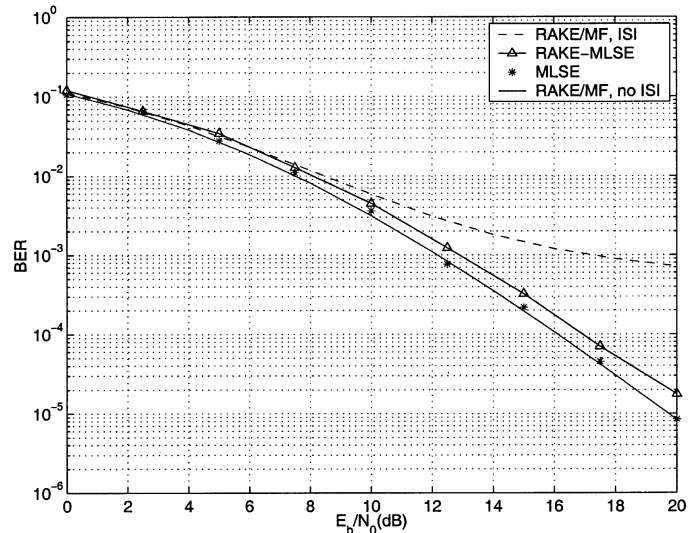


Fig. 11. Comparison of the performance of MLSE receiver with the conventional RAKE receiver (with or without ISI) and the RAKE-MLSE receiver, DS-BPSK signal, three-tap ISI channel, random spreading sequence, $N_s = 4$.

ISI case. However, the MLSE receiver can recover almost all of the loss caused by the ISI with the conventional RAKE receiver. Moreover, the gain of the MLSE receiver over the RAKE-MLSE receiver is more obvious than in the two-tap ISI case, reaching 0.8 dB for $\text{BER} = 1.0 \times 10^{-4}$.

C. Discussion

In Sections V-A and B, two methods are given to evaluate the performance of the MLSE for CDMA signals. The first method,

$$P_b \leq \int_{\alpha_0=0}^{\infty} \int_{\alpha_1=0}^{\infty} \int_{\alpha_2=0}^{\infty} \int_{\theta_1=0}^{\pi} \int_{\theta_2=0}^{\pi} \min \left[\frac{1}{2}, P_b(\alpha_0, \alpha_1, \alpha_2, \theta_1, \theta_2) \right] f_{\alpha_0}(\alpha_0) f_{\alpha_1}(\alpha_1) f_{\theta_1}(\theta_1) f_{\theta_2}(\theta_2) d\theta_1 d\theta_2 d\alpha_2 d\alpha_1 d\alpha_0$$

the eigenanalysis method, evaluates the pairwise error probabilities of simple error events on the fading channel by the eigenvalue decomposition of the path distance matrix, and sums the contributions from a set of simple error events. Usually, the sum is truncated after a certain number of the terms, and so the result is not a strict upper bound. To apply this method to the system with random spreading sequences, the joint density of the random elements in the path distance matrix (e.g., U_1 and U_2 in Section V-B) is required, which may be a lengthy process for large values of L . However, this method allows a clear understanding of the contributions to errors from different error events. In addition, this method can be extended to a time-varying fading channel by considering the correlation function of the fading coefficients [20].

The second method evaluates the conditional bit-error probability by the transfer function of the error-state diagram, and finally, the conditioning is removed by a series of numerical integrations. Usually, a $(2L + 1)$ -fold numerical integration is required for an ISI channel with $L + 1$ taps, and this method cannot be extended to time-varying fading channels. However, a new form of the Gaussian Q -function allows the exact evaluation of the transfer function, and the randomness of the spreading sequence is nicely incorporated. The results obtained are truly upper bounds since no truncation of the sum is performed, and the results may be tighter than those obtained by the eigenanalysis method, due to the minimization of the conditional bit-error probability. Finally, the numerical bound can be easily extended to fading channels with amplitude distributions other than Rayleigh.

VI. CONCLUSION

An MLSE receiver has been proposed for DS signals on a multipath fading channel. The receiver employs a Viterbi decoder which operates on the combined trellis formed by the spreading and the ISI channel, and performs the function of despreading and equalization simultaneously. To evaluate the performance of the receiver, two upper bounds on the bit-error probability have been derived, one using the eigenanalysis method, and the other based upon a numerical technique. Both methods are applied to a multipath Rayleigh fading channel with one or two interfering symbols, when random spreading sequences are used. Comparisons with simulation results show that the analytical bounds are quite accurate. The results also show that significant performance improvement over the conventional RAKE receiver is obtained.

APPENDIX I

DERIVATION OF THE IOWEF OF $1 + D$ ENCODER

In this appendix, we will derive the IOWEF of the $1 + D$ encoder. The input sequence to the encoder is a sequence of i.i.d. binary bits with length N : $\{x_i\}_{i=0}^{N-1}$. The output binary sequence, $\{y_j\}_{j=1}^{N-1}$, is related to the input sequence by $y_i = x_{i-1} \oplus x_i$. The IOWEF is defined by

$$A(W, H) = \sum_{w,h} A_{w,h} W^w H^h$$

where $A_{w,h}$ represents the number of codewords with output weight h generated by input words of weight w . The IOWEF can also be represented by the conditional output weight enumerating function (OWEF)

$$A(W, H) = \sum_w A(w, H) W^w$$

where

$$A(w, H) = \sum_h A_{w,h} H^h.$$

For the trivial cases of $w = 0, N$, we can easily verify that

$$\begin{aligned} A(0, H) &= H^0 \\ A(N, H) &= H^0. \end{aligned}$$

Our derivation follows closely the approach in [21]. Let the all-zero sequence be the reference codeword, and consider an incorrect codeword caused by an input word with weight w . For the $1 + D$ encoder, define a suberror event in the input word as a string of consecutive ones, separated from other suberror events by at least one zero. Each suberror event will contribute two to the output weight h , unless the event is at the edge of the codeword. An input sequence can be uniquely decomposed into m disjoint suberror events, $f_i, i = 1, \dots, m$. There are $\binom{w-1}{m-1}$ distinct decompositions of a sequence of ones with length w into m subsequences, each of length at least one. The number of configurations in which these m subsequences can occur in a word of length N , with consecutive subsequences separated by at least one position, is given by $\binom{N-w+1}{m-1}$. However, we need to consider three cases corresponding to the placement of subsequences with respect to the leading and trailing edges of the word.

1) No subsequence is on the edge.

The output weight $h = 2m, m = 1, 2, \dots, \min(w, N - w - 1)$, and there are $N - w - 1$ possible positions for m subsequences. The conditional OWEF is given by

$$A_1(w, H, m) = \binom{N-w-1}{m} \binom{w-1}{m-1} H^{2m}.$$

2) Only one subsequence is on the edge.

The output weight $h = 2m - 1, m = 1, 2, \dots, \min(w, N - w)$, and there are $N - w - 1$ possible positions for $m - 1$ subsequences not on the edge. The conditional OWEF is given by

$$A_2(w, H, m) = 2 \binom{N-w-1}{m-1} \binom{w-1}{m-1} H^{2m-1}.$$

3) Two subsequences are on the edges.

The output weight $h = 2m - 2, m = 2, 3, \dots, \min(w, N - w + 1)$, and there are $N - w - 1$ possible positions for $m - 2$ subsequences not on the edge. The conditional OWEF is given by

$$A_3(w, H, m) = \binom{N-w-1}{m-2} \binom{w-1}{m-1} H^{2m-2}.$$

Note the two trivial cases are not included in the three cases above. Putting everything together, we obtain the conditional OWEF as

$$A(w, H) = \sum_{m=1}^{\min(w, N-w-1)} A_1(w, H, m) + \sum_{m=1}^{\min(w, N-w)} A_2(w, H, m) + \sum_{m=2}^{\min(w, N-w+1)} A_3(w, H, m)$$

and the IOWEF is given by

$$A(W, H) = W^0 H^0 + W^N H^0 + \sum_{w=1}^{N-1} A(w, H) W^w.$$

APPENDIX II

CONDITIONAL TRANSFER FUNCTION BOUND FOR THE THREE-TAP ISI CHANNEL

In this appendix, we derive the transfer function bound on the conditional bit-error probability $P_b(\alpha_0, \alpha_1, \alpha_2, \theta_1, \theta_2)$ for the MLSE receiver of the random spread signal on a three-tap ISI channel. The transfer function of an error-state diagram with q states is given by [22]

$$T(W, I) = \mathbf{X}(W, I) \mathbf{G}(W, I) \mathbf{Y}(W, I)$$

where

$$\mathbf{G}(W, I) = \sum_{j=0}^{\infty} \mathbf{H}^j(W, I) = [\mathbf{I} - \mathbf{H}(W, I)]^{-1}.$$

Here, the i th element of the row vector $\mathbf{X}(W, I)$ and the column vector $\mathbf{Y}(W, I)$ identify the branch weights of the transition from state 0 to state i and from state i to state 0, respectively. Similarly, the element, $[\mathbf{H}]_{(i,j)}$, of the $(q-1) \times (q-1)$ matrix \mathbf{H} is associated with transition from state i to state j . To numerically evaluate the transfer function bound of the bit-error probability, an explicit expression for $(\partial/\partial I)T(W, I)|_{I=1}$ is given in [22]

$$\frac{\partial}{\partial I} T(W, I)|_{I=1} = \mathbf{X}'(W) \mathbf{G}(W) \mathbf{Y}(W) + \mathbf{X}(W) \mathbf{G}(W) \mathbf{H}'(W) \mathbf{G}(W) \mathbf{Y}(W) + \mathbf{X}(W) \mathbf{G}(W) \mathbf{Y}'(W)$$

where $\mathbf{X}(W)$, $\mathbf{G}(W)$, and $\mathbf{Y}(W)$ are the values of $\mathbf{X}(W, I)$, $\mathbf{G}(s, I)$, and $\mathbf{Y}(W, I)$ evaluated at $I = 1$, and $\mathbf{X}(W)'$, $\mathbf{H}(W)'$, and $\mathbf{Y}(W)'$ are obtained by taking the partial derivatives of $\mathbf{X}(W, I)$, $\mathbf{H}(W, I)$, and $\mathbf{Y}(W, I)$ with respect to I and then evaluating at $I = 1$.

The modified error-state diagram in Fig. 9 can be further simplified to a four-state diagram by preserving the bold-circled states only. The vectors and the matrix are given by

$$\mathbf{X}(W, I) = \left[\frac{1}{2} W^{\beta_0 + \rho_1 + I}, \frac{1}{2} W^{\beta_0 + \rho_1 - I}, 0, 0 \right]$$

$$\mathbf{Y}(W, I) = \left[0, 0, \frac{1}{2} W^{\rho_2 + \beta_5}, \frac{1}{2} W^{\rho_2 + \beta_5} \right]$$

$$\mathbf{H}(W, I) = \begin{bmatrix} 0 & 0 & [\mathbf{T}^{N_s-2}]_{(1,1)} & [\mathbf{T}^{N_s-2}]_{(1,2)} \\ 0 & 0 & [\mathbf{T}^{N_s-2}]_{(2,1)} & [\mathbf{T}^{N_s-2}]_{(2,2)} \\ [\mathbf{T}^2]_{(1,1)} I & [\mathbf{T}^2]_{(1,2)} I & 0 & 0 \\ [\mathbf{T}^2]_{(2,1)} I & [\mathbf{T}^2]_{(2,2)} I & 0 & 0 \end{bmatrix}$$

where $\mathbf{T}(W)$ is the transfer matrix of a simple crossover trellis, given by

$$\mathbf{T}(W) = \frac{1}{2} \begin{bmatrix} W^{\rho_{++}} & W^{\rho_{+-}} \\ W^{\rho_{-+}} & W^{\rho_{--}} \end{bmatrix}.$$

Note these equations can be applied to arbitrary values of N_s , provided that $N_s \geq 2$.

It was shown by Craig [17] that the Gaussian Q -function can be defined by

$$Q(x) = \frac{1}{\pi} \int_0^{\pi/2} \exp\left(-\frac{x^2}{2 \sin^2 \phi}\right) d\phi, \quad x \geq 0. \quad (38)$$

Using this representation, the upper bound on the bit-error probability conditioned on the channel vector is given by [22]

$$P_b \leq \frac{1}{\pi} \int_0^{\pi/2} \frac{\partial}{\partial I} T(W, I)|_{W=\exp(-\gamma_c/4 \sin^2 \phi), I=1} d\phi$$

where $\gamma_c = E_s/N_s N_0$.

The final integral can be efficiently approximated with a Gauss-Chebyshev quadrature formula [23], leading to the following:

$$P_b \leq \frac{1}{2v} \sum_{j=1}^v \frac{\partial}{\partial I} T(W, I)|_{W=\exp(-\gamma_c/4 \sin^2 \phi_j), I=1} + R_v$$

where $\phi_j = (2j-1/4v)\pi$ and R_v is the remainder term. It was shown in [23] that $|R_v| \leq \kappa \gamma_c^{-2v}$ as $\gamma_c \rightarrow \infty$ for some constant κ , and $v = 5$ usually provides sufficient accuracy.

REFERENCES

- [1] "Physical Layer Aspects of UTRA High Speed Downlink Packet Access (Release 4)," 3rd Generation Partnership Project, TR25.848, 3GPP, 2001.
- [2] "Physical Layer Standard for CDMA2000 Spread Spectrum Systems (Release C)," Telecommunications Industry Association, TIA/EIA/IS-2002.2-C, May 2002.
- [3] K. C. Hwang and K. B. Lee, "Performance analysis of low processing gain DS-CDMA systems with random spreading sequences," *IEEE Commun. Lett.*, vol. 2, pp. 315-317, Dec. 1998.
- [4] K. Hooli, M. Juntti, and M. Latva-aho, "Interpath interference suppression in WCDMA systems with low spreading factors," in *Proc. IEEE Vehicular Technology Conf.*, vol. 1, Amsterdam, The Netherlands, Sept. 1999, pp. 421-425.
- [5] S. Tantikovit and A. U. H. Sheikh, "Joint multipath diversity combining and MLSE equalization (RAKE-MLSE receiver) for WCDMA systems," in *Proc. IEEE Vehicular Technology Conf.*, vol. 1, Tokyo, Japan, May 2000, pp. 435-439.
- [6] H. K. Sim and D. G. M. Cruickshank, "A chip-based multiuser detector for the downlink of a DS-CDMA system using a folded state-transition trellis," *IEEE Trans. Commun.*, vol. 49, pp. 1259-1267, July 2001.
- [7] —, "Suboptimum MLSE detector with a folded state-transition trellis preselection stage," *Proc. Inst. Elect. Eng.-Commun.*, vol. 148, pp. 163-168, June 2001.
- [8] G. D. Forney, Jr., "Maximum-likelihood sequence estimation of digital sequences in the presence of intersymbol interference," *IEEE Trans. Inform. Theory*, vol. IT-18, pp. 363-378, May 1972.
- [9] G. Ungerboeck, "Adaptive maximum-likelihood receiver for carrier-modulated data-transmission systems," *IEEE Trans. Commun.*, vol. COM-22, pp. 624-636, May 1974.

- [10] W.-H. Sheen and G. L. Stüber, "MLSE equalization and decoding for multipath-fading channels," *IEEE Trans. Commun.*, vol. 39, pp. 1455–1464, Oct. 1991.
- [11] A. J. Viterbi and J. K. Omura, *Principles of Digital Communication and Coding*. New York: McGraw-Hill, 1979.
- [12] J. G. Proakis, *Digital Communications*, 3rd ed. New York: McGraw-Hill, 1995.
- [13] P. R. Chevillat and E. Eleftheriou, "Decoding of trellis-encoded signals in the presence of intersymbol interference and noise," *IEEE Trans. Commun.*, vol. 37, pp. 669–676, July 1989.
- [14] G. L. Stüber, *Principles of Mobile Communication*. Norwell, MA: Kluwer, 1996.
- [15] E. Malkamäki and H. Leib, "Evaluating the performance of convolutional codes over block fading channels," *IEEE Trans. Inform. Theory*, vol. 45, pp. 1643–1646, July 1999.
- [16] S. A. Raghavan, J. K. Wolf, and L. B. Milstein, "On the performance evaluation of ISI channels," *IEEE Trans. Inform. Theory*, vol. 39, pp. 957–965, May 1993.
- [17] J. W. Craig, "A new, simple, and exact result for calculating the probability of error for two-dimensional signal constellations," in *Proc. IEEE Military Communications Conf.*, vol. 2, McLean, VA, Oct. 1991, pp. 571–575.
- [18] M. B. Pursley, "Performance evaluation for phase-coded spread-spectrum multiple-access communication—part I: System analysis," *IEEE Trans. Commun.*, vol. COM-25, pp. 795–799, Aug. 1977.
- [19] D. L. Noneaker and M. B. Pursley, "The effects of sequence selection on DS spread spectrum with selective fading and RAKE reception," *IEEE Trans. Commun.*, vol. 44, pp. 229–237, Feb. 1996.
- [20] M.-C. Chiu and C.-C. Chao, "Performance of joint equalization and trellis-coded modulation on multipath fading channels," *IEEE Trans. Commun.*, vol. 43, pp. 1230–1234, Feb.-Apr. 1995.
- [21] M. Öberg and P. H. Siegel, "Performance analysis of turbo-equalized diode partial-response channel," *IEEE Trans. Commun.*, vol. 49, pp. 436–444, Mar. 2001.
- [22] J. K. Cavers, J.-H. Kim, and P. Ho, "Exact calculation of the union bound on performance of trellis-coded modulation in fading channels," *IEEE Trans. Commun.*, vol. 46, pp. 576–579, May 1998.
- [23] C. Tellambura, "Evaluation of the exact union bound for trellis-coded modulations over fading channels," *IEEE Trans. Commun.*, vol. 44, pp. 1693–1699, Dec. 1996.



Kai Tang (S'98–M'92) received the B.S. and M.S. degrees in electrical engineering from Southeast University, Nanjing, China, in 1994 and 1997, respectively. He received the Ph.D. degree in electrical engineering from University of California, San Diego, in 2001.

He is currently a Senior Engineer with Qualcomm Inc., San Diego, CA, where he participated in the design, simulation, and implementation of wireless communications and location positioning ASICs.



Laurence B. Milstein (S'66–M'68–SM'77–F'85) received the B.E.E. degree from the City College of New York, New York, NY, in 1964, and the M.S. and Ph.D. degrees in electrical engineering from the Polytechnic Institute of Brooklyn, Brooklyn, NY, in 1966 and 1968, respectively.

From 1968 to 1974, he was with the Space and Communications Group of Hughes Aircraft Company, and from 1974 to 1976, he was a member of the Department of Electrical and Systems Engineering, Rensselaer Polytechnic Institute, Troy, NY. Since 1976, he has been with the Department of Electrical and Computer Engineering, University of California at San Diego, La Jolla, where he is a Professor and former Department Chairman, working in the area of digital communication theory with special emphasis on spread-spectrum communication systems. He has also been a consultant to both government and industry in the areas of radar and communications.

Dr. Milstein was an Associate Editor for Communication Theory for the IEEE TRANSACTIONS ON COMMUNICATIONS, an Associate Editor for Book Reviews for the IEEE TRANSACTIONS ON INFORMATION THEORY, an Associate Technical Editor for the *IEEE Communications Magazine*, and the Editor-in-Chief of the IEEE JOURNAL ON SELECTED AREAS IN COMMUNICATIONS. He was the Vice President for Technical Affairs in 1990 and 1991 of the IEEE Communications Society, and has been a member of the Board of Governors of both the IEEE Communications Society and the IEEE Information Theory Society. He is a former member of the IEEE Fellows Selection Committee, and a former Chair of ComSoc's Strategic Planning Committee. He is a recipient of the 1998 Military Communications Conference Long Term Technical Achievement Award, an Academic Senate 1999 UCSD Distinguished Teaching Award, an IEEE Third Millennium Medal in 2000, the 2000 IEEE Communication Society Armstrong Technical Achievement Award, and the 2002 MILCOM Fred Ellersich Award.



Paul H. Siegel (M'82–SM'90–F'97) received the S.B. degree in 1975 and the Ph.D. degree in 1979, both in mathematics, from the Massachusetts Institute of Technology, Cambridge.

He was with the IBM Research Division from 1980 to 1995. He joined the Faculty of the School of Engineering, University of California, San Diego, in July, 1995, where he is currently Professor of Electrical and Computer Engineering. He is affiliated with the Center for Wireless Communications and became Director of the Center for Magnetic Recording Research in September, 2000. His primary research interest is the mathematical foundations of signal processing and coding, especially as applicable to digital data storage and communications. He holds several patents in the area of coding and detection for digital recording systems.

Dr. Siegel was a corecipient of the 1992 IEEE Information Theory Society Paper Award and the 1993 IEEE Communications Society Leonard G. Abraham Prize Paper Award. He held a Chaim Weizmann Fellowship during a year of postdoctoral study at the Courant Institute, New York University, New York. He was a member of the Board of Governors of the IEEE Information Theory Society from 1991 to 1996. He served as Co-Guest Editor of the May 1991 Special Issue on "Coding for Storage Devices" of the IEEE TRANSACTIONS ON INFORMATION THEORY, of which he is currently Editor-in-Chief, and was an Associate Editor for Coding Techniques from 1992 to 1995. He is a member of Phi Beta Kappa.